

SENSITIVITY ANALYSIS OF PLUG FLOW PORE SURFACE DIFFUSION MODEL PART II: FOR MULTICOMPONENT

Seongho Hong[†]

Department of Chemical and Environmental Engineering, Soongsil University, Seoul, Korea
(received November 2003, accepted February 2004)

Abstract : For a multicomponent solution, such as NOM, which contains components of various adsorbabilities, the homogeneous surface diffusion model (HSDM) may be unable to accurately predict the adsorption process since it does not consider pore diffusion. Due to the competition between the weakly and strongly adsorbing components in the mass transfer zone, pore diffusion may be the dominant intraparticle mass transfer mechanism for the weakly adsorbing components in a fixed bed adsorbers. In this study, a sensitivity analysis was performed to determine which parameters have the greatest impact on the model results for a multicomponent mixture, like NOM. The fictive component ratio was an important parameter in determining the breakthrough pattern. When the solution contained more strongly adsorbable component the fixed bed life was extended. Also, the initial concentration was important, yielding much shorter run times with increasing concentrations. The SPDFR and tortuosity also had a great impact on the breakthrough pattern for multicomponent solutions, while the molecular weight was found not to be important in the range found for natural waters. The backwashing impact on the breakthrough pattern of multicomponent solutions was not significant for the NOM conditions tested.

Key Words : GAC, Adsorption, multicomponent, NOM, IAST

INTRODUCTION

For a multicomponent solution, such as NOM, which contains components of various adsorbabilities, the homogeneous surface diffusion model (HSDM) may be unable to accurately predict the adsorption process since it does not consider pore diffusion. The surface loading of the weakly adsorbing components may be small compared to the strongly adsorbing components. Due to the competition between the weakly and strongly adsorbing components in the mass transfer zone, pore diffusion may be the dominant intraparticle mass transfer mechanism for

the weakly adsorbing components in a fixed bed adsorbers. The weakly adsorbing components are important as they breakthrough first and can determine the adsorber run time if a low effluent criteria is used. Therefore, the pore diffusion needs to be considered when predicting multicomponent adsorption in the fixed bed adsorber.¹⁾

The plug-flow pore-surface diffusion model (PFPSDM), which incorporates both pore and surface diffusion as mass transfer mechanisms, was developed to predict fixed bed adsorber breakthrough behavior with mixtures of known components using the equilibrium and kinetic parameters of each component in the mixture.²⁾ The PFPSDM has also been used to describe the NOM breakthrough behavior using equili-

[†] Corresponding author

E-mail: shong@ssu.ac.kr

Tel: +82-2-820-0628, Fax: +82-2-812-5378

brum and kinetic parameters of fictive components in the fixed bed adsorber.³⁾ For this study, the PFPSDM was used to predict NOM breakthrough.

The kinetic parameters used in the PFPSDM were assumed to be identical for all fictive components because their liquid diffusivities were assumed to be same for all fictive components.³⁾ Fettig and Sontheimer⁴⁾ have shown that when the PFPSDM is used only the intraparticle diffusion coefficient of the strongly adsorbing components can be determined.

In this study, a sensitivity analysis was performed to determine which parameters have the greatest impact on the model results for a multicomponent mixture, like NOM. The parameters used in this study include: molecular weight, surface pore diffusion flux ratio (SPDFR), tortuosity (τ), adsorbability and backwashing frequency for a single component, and total DOC concentration, composition of fictive components, tortuosity, SPDFR and molecular weight for a multicomponent solution. Also, impact of the parameters was investigated on backwashing condition.

MODEL DEVELOPMENT FOR THE PFPSDM

The assumptions incorporated into the PFPSDM are as follows: 1) the liquid phase flux is described by the linear driving force approximation, 2) the adsorption rate is very fast (local equilibrium), 3) the multi-component adsorption equilibria are described by the single solute Freundlich isotherm equation and IAST, 4) surface and pore diffusion describe the intraparticle mass flux and are independent of concentration, 5) there are no solute-solute interactions in the diffusion process, 6) the adsorbent particle is spherical, 7) solute transport in the axial direction occurs by advective flow, and 8) there is no radial dispersion or channeling.

The mass balance can be expressed in mathematical terms as follows:

$$\begin{aligned} & \varepsilon v A [C_i(z, t) - C_i(z + \Delta z, t)] \Delta t \\ & - \varepsilon A D_{e,i} \left[\frac{\partial C_i(z, t)}{\partial z} - \frac{\partial C_i(z + \Delta z, t)}{\partial z} \right] \Delta t \\ & = \varepsilon A [C_i(z, t + \Delta t) - C_i(z, t)] \\ & + p_a (1 - \varepsilon) A [q_{avg,i}(z, t + \Delta t) - q_{avg,i}(z, t)] \\ & \left[+ \frac{\varepsilon_p}{P_a} C_{p,avg,i}(z, t + \Delta t) - \frac{\varepsilon_p}{P_a} C_{p,avg,i}(z, t) \right] \Delta z \end{aligned} \tag{1}$$

in which, ε is the bed porosity; v is the interstitial velocity; ε_p is the void fraction of the pores within the adsorbent; A is the cross sectional area of the differential element; $C_i(z,t)$ is the liquid phase concentration of component i ; $D_{e,i}$ is the axial eddy dispersivity based on the interstitial velocity of component i ; P_a is the adsorbent density; $q_{avg,i}(z,t)$ is the average adsorbent phase concentration of component i ; $C_{p,avg,i}$ is the average adsorbate concentration of component i in the adsorbent pores; z is the axial coordinate; and t is the elapsed time.

The total average adsorbent phase concentration is given by;

$$\begin{aligned} & q_{avg,i}(z, t) + \frac{\varepsilon_p}{P_a} C_{p,avg,i}(z, t) \\ & = \frac{3}{R^3} \int_0^R \left[q_i(r, z, t) - \frac{\varepsilon_p}{P_a} C_{p,i}(r, z, t) \right] r^2 dr \end{aligned} \tag{2}$$

in which, R is the radius of the adsorbent; and r is the radial coordinate.

Dividing Eq. 1 by $A \Delta z \Delta t$ and taking the limits as Δz and Δt approach zero and substituting the Eq. 2 into Eq. 1 yield Eq. 3. Eq. 3 is the final form of the overall mass balance for component i in the fixed bed adsorber.

$$\begin{aligned} & -V\varepsilon \frac{dC_i(z, t)}{dz} + \varepsilon D_{e,i} \frac{d^2 C_i(z, t)}{dz^2} = \\ & \varepsilon \frac{dC_i(z, t)}{dt} + \frac{3p_a(1-\varepsilon)}{R^3} \frac{\partial}{\partial t} \int_0^R \\ & \left[q_i(z, r, t) + \frac{\varepsilon_p}{P_a} C_{p,i}(r, z, t) \right] r^2 dr \end{aligned} \tag{3}$$

The dispersion term in Eq. 3 can be neglected

based on initial model assumptions. Thus, Eq. 3 becomes a first order partial derivative with respect to z . In order to solve Eq. 3, one initial condition and one boundary condition are needed. The initial and boundary conditions are as follows:

$$C_i(0 \leq x \leq L, t = 0) = 0 \quad (4)$$

$$V[C_o - C_i(z = L, t)] = \frac{\partial}{\partial t} \left[\int_0^L \left[C_i(z, t) + \frac{3p_a(1-\epsilon)}{\epsilon R^3} \right] \int_0^R \left[q_i(r, z, t) + \frac{\epsilon_p}{\rho_a} C_{p,i}(r, z, t) r^2 dr \right] dz \right] \quad (5)$$

The liquid phase mass balance for component i is derived using the same differential element used in the previous development. The final form of the liquid phase mass balance for component i in the fixed bed adsorber is:

$$-v \frac{dC_i(z, t)}{dz} + D_{e,i} \frac{d^2 C_i(z, t)}{dz^2} = \frac{dC_i(z, t)}{dt} + \frac{3\beta_L(1-\epsilon)}{R\epsilon} [C_i(z, t) - C_{p,i}(r = R, z, t)] \quad (6)$$

in which, $C_{p,i}(r=R, z, t)$ is the adsorbate phase concentration of component i at the adsorbent surface and β_L is the external mass transfer coefficient. The final form of the intraparticle mass balance is given by Eq. 7.

$$\frac{1}{r^2} \frac{\partial}{\partial r} [r^2 D_{s,i} \frac{\partial q_i(r, z, t)}{\partial r} + r^2 \frac{D_{p,i} \epsilon_p}{\rho_a} \frac{\partial C_{p,i}(r, z, t)}{\partial r}] = \frac{\partial}{\partial t} [q_i(r, z, t) + \frac{\epsilon_p}{\rho_a} C_{p,i}(r, z, t)] \quad (7)$$

in which, $D_{s,i}$ is the surface diffusion coefficient and $D_{p,i}$ is the pore diffusion coefficient of component i . The initial condition for Eq. 7 is:

$$(q_i + \frac{\epsilon_p}{\rho_a} C_{p,i})(0 \leq r \leq R, 0 \leq z \leq L, t = 0) = 0 \quad (8)$$

The following equations are the boundary

conditions for Eq. 7.

$$\frac{\partial}{\partial r} [(q_i + \frac{\epsilon_p}{\rho_a} C_{p,i})(r = 0, 0 \leq z \leq L, t = 0)] = 0 \quad (9)$$

$$\frac{\partial}{\partial t} \int_0^R [q_i(r, z, t) + \frac{\epsilon_p}{\rho_a} C_{p,i}(r, z, t)] r^2 dr = \frac{k_{f,i} R^2}{\rho_a} [C_i(z, t) - C_{p,i}(r = R, z, t = 0)] \quad (10)$$

The nonlinear equation which couples the liquid and intraparticle mass balances is the Freundlich isotherm equation; $q = KC^n$. Applying the IAST, the final result including the axial coordinate for the concentration of a multi-component is given by:

$$C_{p,i}(r, z, t) = \frac{q_i(r, z, t)}{\sum_{j=1}^N q_j(r, z, t)} \left(n_i \frac{\sum_{j=1}^N q_j(r, z, t)}{K_i} \right)^{\frac{1}{n_i}} \quad (11)$$

The pore diffusion coefficient is defined by Eq. 12 where τ is the tortuosity.

$$D_p = \frac{D_L \epsilon_p}{\tau} \quad (12)$$

in which D_L is the liquid diffusivity. The surface diffusion coefficient, D_s , is a function of the empirically determined surface pore diffusion flux ratio (SPDFR).

$$D_s = \frac{D_L \epsilon_p C_0 \text{ SPDFR}}{KC_0^n} \quad (13)$$

When the SPDFR is much greater than 1.0 the dominant intraparticle mechanism is surface diffusion. When it is much less than 1.0, pore diffusion dominates. When the SPDFR is 1.0 there is no dominant intraparticle mechanism, i.e. surface diffusion and pore diffusion equally contribute.

BACKWASHING MODEL DEVELOPMENT

Backwashing model for multicomponent is very similar to that of single component. Therefore, after backwashing each axial coordinate will have the same radial concentration gradient for each adsorbable component. The Eq. 14 and 15 which were described in part I was used for backwashed condition. However, the solid phase concentration of each fictive component was calculated based on the Eq. 14 in the part I. Also, the liquid phase concentration after backwashing was set to the influent concentration of each fictive component.

RESULTS AND DISCUSSION

The parameters and their starting values for a multicomponent, such as NOM, are listed in Table 1. Initial parameter values were obtained from previous studies.^{5,6)} In this study, the fictive components are divided based on the K values of Freundlich isotherm.

Table 1. Input Parameters and Initial Values for Multicomponent Sensitivity Analysis

C0	Tortuosity	SPDFR	FCD*	MW*
mg/L	-	-	-	daltons
6.0	7.0	0.1	10:10:15:65	2250

FCD* : Fictive component distribution (K= 0,10,25,50)

MW* : Molecular weight

n = 0.2

Figure 1 shows the impact of fictive component composition at the same initial total DOC concentration. The concentration distribution of the fictive component fractions was varied similar to that of occurring in natural waters. The non-adsorbable fraction (K=0) was fixed at 10 percent of the initial total DOC concentration. When the solutions contained the large amounts of the weakly adsorbable fraction (cases I and II), the breakthrough patterns showed a similar trend up to the 40 percent breakthrough point. After that point, the breakthrough was

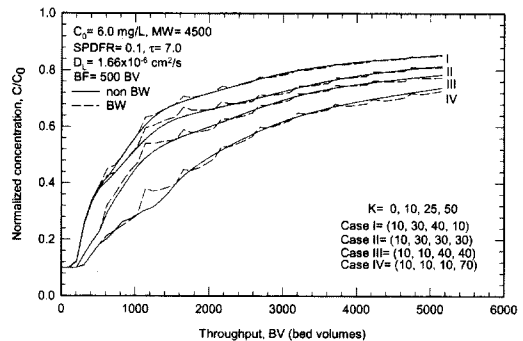


Figure 1. Impact of fictive component ratio on multicomponent solution breakthrough.

dictated by the mid- adsorbable and strongly adsorbable fractions. The increasing the amount of the strongly adsorbable fraction in the multicomponent solution, yielded the later breakthrough.

As seen for the single solute sensitivity analysis, each fictive component of the multicomponent solution broke through earlier in the backwashed column compared to the adsorption column. For the multicomponent solution, the earlier breakthrough can be caused by two different reasons; one is the reverse of the concentration gradient and the other is displacement of the weakly adsorbable components on the adsorbent by the strongly adsorbable components. However, the backwashing impact for the multicomponent solution was not significant compared to that for the single component because the breakthrough of each fictive component was staggered and when summed together, the fictive components behavior at different degrees of breakthrough compensated for the early breakthrough. Thus, further sensitivity analysis for the multicomponent solution was not performed with the backwashed column model.

Figure 2 shows the breakthrough of each fictive component for natural groundwater. The overall breakthrough was divided into three fictive components based on K values. The lower the K values showed the earlier breakthrough. However, the impact of backwashing was smaller in overall breakthrough than those

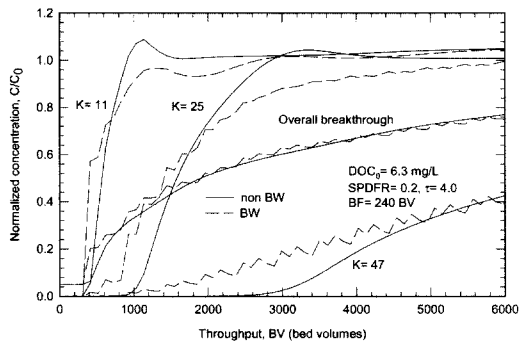


Figure 2. Fictive component breakthrough for natural groundwater.

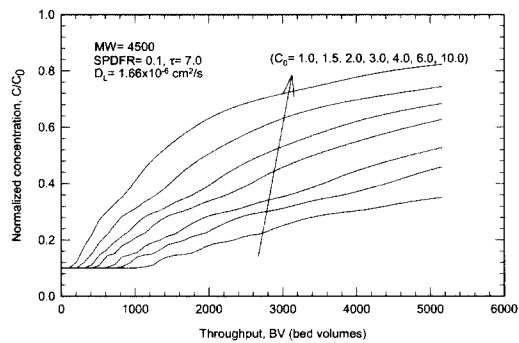


Figure 3. Impact of initial concentration on multicomponent solution breakthrough.

in each fictive component.

Figure 3 shows the impact of initial total DOC concentration at same fictive component ratio. The initial DOC concentration was varied from 1.0 to 10.0 mg/L, which is representative of treated drinking waters. The impact of initial DOC concentration can be clearly seen from the graph. As the initial concentration was increased, performance decreased as indicated by shorter run time to 50 percent breakthrough.

Figure 4 shows the impact of tortuosity on PFPSPDM breakthrough pattern. The tortuosity was varied from 1.0 to 10.0. When the tortuosity was 1.0, there was no breakthrough until 1,000 BV. When the tortuosity is 1.0 the diffusion path is same as the particle radius. The impact of tortuosity on breakthrough pattern of a multicomponent solution was very different compared to that of a single component which was on Figure 6 in part I. The shape of the

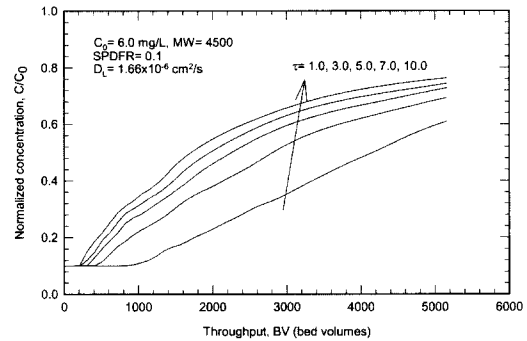


Figure 4. Impact of tortuosity on multicomponent solution breakthrough.

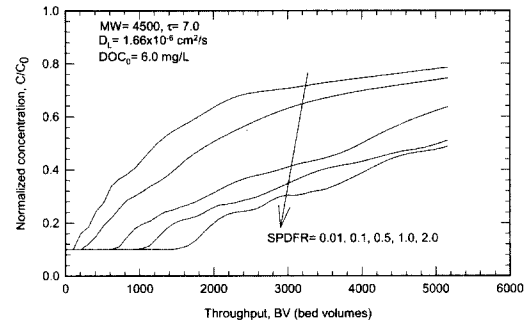


Figure 5. Impact of SPDFR on multicomponent solution breakthrough.

breakthrough pattern was not as affected by varying the tortuosity, however, the time to 60 percent breakthrough was extended by decreasing the tortuosity. The effluent concentrations of the $\tau=10$ and $\tau=1$ runs were equal at 85 percent breakthrough, after which the breakthrough for $\tau=1$ was higher.

Figure 5 shows the impact of the SPDFR on breakthrough for a multicomponent. The SPDFR was varied from 0.01 to 2.0, i.e., the dominant mass transfer mechanism was varied from being 99 percent pore diffusion to 67 percent surface diffusion. The initial breakthrough was extended by increasing the SPDFR, i.e., surface diffusion domination. Also, when the SPDFR was greater than 0.5 the program started to show instability for these adsorption conditions. Most of the natural waters could be simulated a SPDFR of 0.3.

The molecular weight impact for the multicomponent solution breakthrough is shown in

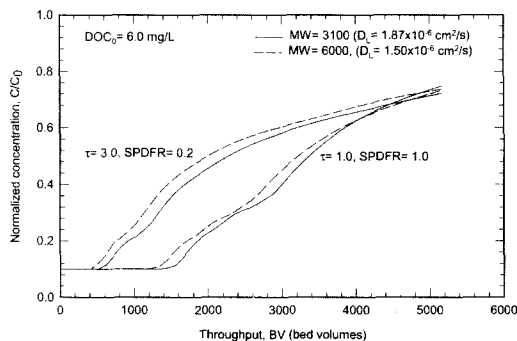


Figure 6. Impact of molecular weight on multicomponent solution breakthrough.

Figure 6. The graph shows the impact for two different molecular weights at two different conditions. Even though the molecular weights were varied as much as a factor of 2, the impact on the breakthrough was less than 5 percent for both conditions and molecular weights.

CONCLUSIONS

The fictive component ratio was an important parameter in determining the breakthrough pattern. When the solution contained more strongly adsorbable component the fixed bed life was extended. Also, the initial concentration was important, yielding much shorter run times with increasing concentrations. The SPDFR and tortuosity, also had a great impact on the breakthrough pattern for multicomponent solutions, while the molecular weight was found not to be important in the range found for natural waters. The backwashing impact on the breakthrough pattern of multicomponent solutions was not significant for the NOM conditions tested. This was due to staggered breakthrough of each

fictive component and when summed together the fictive component concentrations compensate for each other.

ACKNOWLEDGMENT

This research was supported by internal research fund of Soongsil University.

REFERENCES

1. Friedman, G., "Mathematical Modeling of Multicomponent Adsorption in Batch and Fixed-Bed Reactors," MS Thesis, Michigan Technological Univ. Ann Arbor, Michigan, US (1984).
2. Crittenden, J. C., Luft, P., and Hand, D.W., "Prediction of Multicomponent Adsorption Equilibria in Background Mixtures of Unknown Composition," *Water Res.*, **19**(12), pp. 1537~1548 (1985).
3. Sontheimer, H., Crittenden, J. C., and Summers, R., "Activated Carbon for Water Treatment," DVGW Forschungsstelle, Karlsruhe, Germany (1988).
4. Fettig, J. and Sontheimer, H., "Kinetics of adsorption on activated carbon: II. multi-solute systems," *J. of Environ. Eng.*, **113**(4), pp. 780~794 (1987).
5. Hong, S., "Activated Carbon Adsorption of Organic Matter: Backwashing, Desorption and Attenuation," Ph.D Diss. University of Cincinnati, Ohio, US (1995).
6. Hong, S., "The Role of pH and Initial Concentration on GAC Adsorption for Removal of Natural Organic Matter," *J. of Environ. Eng. Res.*, **3**(4), 183~190 (1998).